# A Verification of the POP model within CCSM2

## Can changes of Ocean Climate be detected?

**by**

**Anders Aaman**

***Master Thesis in Geosciences***

***Physical Oceanography***


*Department of Geosciences*
*Faculty of Mathematics and Natural Sciences*

*December 2006*

*UNIVERSITY OF OSLO*

# Contents

# List of Figures

# 1 Abstract

A control run of 150 years for CCSM2 has been performed at the Norwegian Meteorological Institute. In this run the external forcing(especially radiation) were held constant, $CO_2$ were held at the level of 1990. $CO_2$ influences only the atmosphere and the the carbon cycle between ocean and atmosphere is not included. Both ocean, ice, and atmosphere will vary as a function of time in this run, although we might not be able to compare model data directly with the observed data, it is however possible to observe variations in atmospheric climate, extension of the SST, ocean circulation, and ocean hydrography(which is the most common type of data that we have, both modern as well as paleo data).What we are most interested in is to investigate the role of the meridional ocean circulation in this system, as variations of it often is used as a measure of the role the ocean circulation might have in this system.

The survey should be started on a more global scale and should thereafter be expanded to a smaller scale, which means of dividing this up into boxes. In this document we will especially focus ourselves on the subtropical and mid-latitude part of the Atlantic sector, where the meridional circulation and heat transport is the greatest. We will be considering the following:

- SST, SSS
- Mean Ocean temperature
- Mean Salinity
- Comparisons of temperature for Lev/POP
- Temperature Anomalies
- SST Anomalies
- Volume and Heat transports.

# 2 Introduction

In the climatology project RegClim the global, fully coupled climatology model CCSM2 from NCAR is run in cooperation with the University of Oslo and the Norwegian Meteorological Institute. The aim is primary to study what effect coupling from aerosols and soot have on the climate

and the circulation pattern in the atmosphere. These experiments has not started yet, but control simulations are performed with the coupled model system in order to familiarise oneself with its functions before new processes are introduced.The results from these simulations gives excellent opportunities for analysis of data from a very advanced system of climate models, where there is full interaction between the different model components. The model does not use artificial corrections for the flux in order to give a more stable and realistic climate. It therefore gives a consistent and according to present standard a reasonably realistic description of the interaction between ocean and atmosphere in northern latitudes. The data from the control run should be analysed in order to study the exchange between ocean and atmosphere in the northern Atlantic and the Arctic.
The data in question has been modelled over a period of 150 years. This run is done with the radiation and the composition of the atmosphere according to the values that existed in 1990. Otherwise the model is at liberty to develop on its own. Comparisons should then be done with variability and mean data. The model has a resolution of about 2.8 degrees for the atmosphere, and about 1 degree for the ocean. For the Nordic Seas the resolution is about 60-70 km. Known problems for the model is: it is too warm in the Nordic Seas, too warm over land in the winter, and the ice is too thin during winter.

# 3 Aim

The focus of this master thesis is to verify the POP model within CCSM2 from NCAR and when possible compare data/results with observations, which is represented by the Levitus series, that can be loaded down from the Internet, but has been supplied to the author as netCDF files in this case.
A further aim of the thesis is to establish or at least indicate what impact the results will or might have on ocean climate.
In order to simplify the analysis, a number transects have been created showing temperature and salinity values at selected latitudes.
Total temperature and SST anomalies from the model have been looked at and investigated as well.
When analysing the volume and heat transports, data from WOCE (World Ocean Circulation Experiment) are also referred to.
Calculations of heat and volume transports from the equator to 60 °N have been done.

# 4 Ocean Processes and Climate-An Overview

The characteristic of complex systems is their ability to develop transient structures when reacting to internal and external forcing as a result of their internal non-linear dynamics.
Examples of this is the atmosphere, ocean, and different ecosystems.

## 4.1 Approach to complex climate systems

In order to prove or show this the approach from a scientific point of view experiments are used.
Within the geosciences this creates a certain difficulty, where deliberate experiments are impossible, the approach is here via more long-term close to global observations that might lead to a certain degree of understanding that then will then make allowance for numerical predictions on a more restricted time scale.
A good example of this approach is within weather forecasting. It should be mentioned that weather forecasting can only be successful up to a time scale of about two weeks and at present does not include more from the ocean than SST as a starting point for the conclusive prediction up to a week in advance. The climate system displays some statistical stability over the long term despite reacting to conclusive instability to changed initial conditions.

## 4.2 Ocean-Atmosphere interaction

The ocean and atmosphere transport about the same amount of heat from low to high latitudes. It is however achieved in very different ways. In the atmosphere it is done primarily by transient eddies in the middle and high latitudes. In the ocean on the other hand, boundary currents, large gyres (wind-driven to a large extent), and the vertical overturning will responsible for this process.
Even if the sun delivers more energy to the southern hemisphere, the northern hemisphere nevertheless contains the thermal equator at all seasons over the Atlantic and the Pacific. The reason for with regards to the Atlantic is the shape of South America and Africa and that the ocean in question transports about 1 PW of heat across the equator into the northern hemisphere. Although the ocean is influenced by the atmosphere through fluxes of momentum, fresh water, incoming solar irradiance and atmospheric thermal radiation, SST is the main parameter influencing the heat fluxes from the ocean to the atmosphere. The results of these ocean

influences, are reduced seasonal variation in maritime areas as compared with continental regions, which means weaker meridional gradients and strong longitudinal dependence of yearly average temperatures, especially in the North Atlantic.
A major reason for these temperatures (apart from heat transport from the subtropical Atlantic) is the high salinity in the northern latitude Atlantic leading to intermittent deep convection events either near the sea-ice edge or in the open ocean.
Long-term mean ocean-atmosphere interactions are responsible for the mean differences between marine and continental climates. Internal variability of the atmosphere-ocean-cryosphere climate system on all time scales, supplemented by external forcing produces the observed climate variability. On very long time scales, the forcing by the changed orbit of the earth around the sun (Milankovitch cycles) become dominant.

## 4.3 Cryosphere and the oceans

Ice-ocean interactions are an important part of the climate system. Mountain glaciers, small ice caps and ice sheets influence the global sea level. Deep convection in the Arctic and the Southern Oceans is largely related to sea-ice formation on continental shelves and open ocean convection is often caused by atmospheric forcing at the sea-ice edge. Sea ice is treated interactively in most coupled ocean-atmosphere models and improved parameterisations for dynamical sea-ice behaviour have also been selected in CCSM.
The positive freshwater balance of the Arctic Ocean creates a thin and cold, less saline layer on top of a much warmer and more saline intermediate layer of Atlantic origin. Then heat content of this deeper layer is sufficient to melt the entire multi year sea ice. Therefore, changes in the salinity of the top layer through changes in Arctic river runoff, snow-depth on sea ice and evaporation could have strong impact on Arctic sea ice, in turn on Arctic Ocean circulation and at least on regional climate. However, the observation of solid precipitation is at present not adequate to detect changes. This is because earlier observations (for example, snow depth on sea ice measured regularly in spring at many stations where ocean profiling has taken place) have largely ceased following the collapse of the Soviet Union. As yet, remote sensing methods of sufficient accuracy to detect these precipitation changes have not been developed.

## 4.4 Anthropogenic climate change and the oceans

The ocean as a key component of the climate system also plays a major role in anthropogenic climate change. First, ocean heat absorption delays the full global warming. Second, the oceans, particularly their regional pattern of heat transport and absorption, lead to significant changes in regional climate and thus rainfall and temperature change. Third, the oceans are a major sink for anthropogenic carbon dioxide. Fourth, ocean heat absorption leads to thermal expansion of the oceans and sea level elevation, which results in coastal erosion and flooding. Fifth, changes in the formation of deep water masses at high latitudes in the North Atlantic and the Southern Ocean could lead to abrupt changes in the global ocean thermohaline or MOC circulation and a major rearrangement of global climate.
The warming response is dependent on the rate of increase of the greenhouse gases because of the uptake of heat by the oceans. The present rate of increase of greenhouse gas concentration is below 1 percent per year, accounting for the combined effect of all greenhouse gases. Thus only about 60 percent of the warming we are committed to because of increases in past greenhouse gas concentration should have been realised to date. In addition to slowing the rate of warming, changes in precipitation patterns will depend strongly on the warming pattern of the ocean.
The ocean water contains about 50 times the carbon stored in the atmosphere. On average about 90 billion tons of carbon (GtC) are released from the ocean and about 92 GtC are absorbed by the ocean each year.
Mean sea-level rise is one of the major consequences of anthropogenic climate change. While the further melting of land ice will certainly lead to sea-level rise, thermal expansion of seawater will be the dominant contribution during the twenty-first century. Sea-level rise threatens the coastal zone where most of the world population lives, especially those zones where there may be concomitant increases in storm surges. Thus sea-level rise is a major argument in the political debates on anthropogenic climate change.

# 5 The Model

The Community Climate System Model (CCSM) is a coupled climate model that simulates the Earth's Climate System. It is composed of four separate model components simultaneously simulating the atmosphere, ocean, land , and sea-ice, and additionally it consists of a coupling component, CCSM allows scientists and others to conduct important research into the

the earths past, present, and future climate.
There exists both high low resolution versions within CCSM. A high resolution version is well suited in order to model climates within 100-150 years or so. It is therefore quite well suited for our purposes in this thesis. Low resolution versions is better suited for paleoclimate and debugging.
The system is supported by the National Science Foundation (NSF) and located at the National Centre for Atmospheric Research (NCAR) in Boulder, Colorado.

## 5.1 POP

Regarding the version used in this document, CCSM consists of four components: The Coupler, The Atmospheric Component, The Ocean Component (OCN), The Sea-Ice Component, The Land-Surface Component. Each component will then have a model associated with it, which pertains to the environment in question.
Both full dynamical model and data-cycling versions are supplied for each model component. The CCSM is written in Fortran 90, which is a compiler that will enhance the systems performance.
POP was developed at LANL (Los Alamos National Laboratory) under the sponsorship of the US Department of Energy's CHAMMP program, which brought massively parallel-computers into the the field of modelling. POP is a descendant of the Bryan-Cox-Semtner (BCS) class of models. A number of improvements have been developed and incorporated into POP. Although originally motivated by the adaptation of POP for massively parallel computers, many of these changes has improved not only its computer performance but the probability of the model's physical representation of the real ocean as well.
The barotropic streamfunction in the standard BCS models has required an additional equation to be solved for each continent and island that penetrates the ocean surface. This has been costly even on machines like Cray parallel-vector-processor computers, which has a fast memory access. To reduce the number of equations to solve with the barotropic streamfunction, it has been common practise to submerge islands, connect them to nearby continents with artificial land bridges, or to merge an island chain into a single mass without gaps. The first modification created artificial gaps, permitting increased flow, while the latter closed channels that could exist.
On distributed-memory parallel computers, these added equations were even more costly because each required the gathering of data from an arbi-

trarily large set of processors to perform a line-integral around each landmass. This computational dilemma was addressed by developing a new set up for the barotropic mode based on surface pressure. The boundary condition for the surface pressure at a land-ocean interface point is local, which eliminates the non-local line-integral.
As a consequence, the surface-pressure permits any number of islands to be included at no additional computational cost, so all channels can be treated as precisely as the resolution of the grid permits.
An additional concern with the barotropic streamfunction is that the elliptic equation to be solved is ill-conditioned if the bottom topography has large spatial gradients. The bottom topography must be smoothed to maintain numerical stability. Although this reduces the fidelity of the simulation, it does have the 'desirable' side effect (given the other limitations of the streamfunction approach mentioned above) of submerging many islands, thereby reducing the number of equations to be solved. In contrast, the surface-pressure definition allows more realistic, smoothed bottom topography to be used with no reduction in the time step.
An implicit free-surface boundary condition that allows the air-sea interface to evolve freely and allows the sea-surface height to be used as prognosis, is implemented in POP. Optionally, the top-most layer thickness is allowed to change, thus permitting natural freshwater flux boundary conditions.
Scaling of the horizontal diffusion coefficient by $(\cos(j))^n$ was introduced, where j is latitude and n=1 for Laplacian mixing and n=3 for bi-harmonic mixing. This optional scaling prevents horizontal diffusion from limiting the time step severely at high latitudes, yet keeps diffusion large enough to maintain numerical stability.
After the temperature and salinity have been updated to time-step n+1 in the baroclinic routines, the density $\rho^{n+1}$ and pressure $p^{n+1}$ can be computed. By computing the pressure gradient with a linear combination of p at three time-levels (n-1, n, and n+1), a technique well known in atmospheric modelling (Brown and Campana, 1978), it is possible to increase the time-step by as much as a factor of two, if the internal gravity waves are the controlling factor.
Because the code is written in Fortran 90, it was relatively easy to reformulate and discretetise the equations of motion to allow the use of any locally orthogonal horizontal grid. This provides alternatives to the standard latitude-longitude grid with its singularity at the North Pole.
This generalisation made possible the development of the displaced-pole grid, which moves the singularity arising from convergence of meridians at the North Pole into an adjacent landmass such as North America, Rus-

sia or Greenland. This leaves a smooth, singularity-free grid in the Arctic Ocean. That grid joins smoothly at the equator with a standard Mercator grid in the Southern Hemisphere.

### 5.1.1 Detailed Overview

Like all models POP is based on the normal momentum equations, and have then been modified from them. A numerical scheme has then been employed in order to solve our possible problems.

*Momentum and primitive equations*

The equations that we use in our discussion are: the momentum, continuity, and density.

x-momentum:

$$\frac{\partial u}{\partial t} + u\frac{\partial u}{\partial x} + v\frac{\partial u}{\partial y} + w\frac{\partial u}{\partial z} - fv = -\frac{1}{\rho_0}\frac{\partial p}{\partial x} + \nu\frac{\partial^2 u}{\partial z^2} \tag{1}$$

y-momentum:

$$\frac{\partial v}{\partial t} + u\frac{\partial v}{\partial x} + v\frac{\partial v}{\partial y} + w\frac{\partial v}{\partial z} + fu = -\frac{1}{\rho_0}\frac{\partial p}{\partial y} + \nu\frac{\partial^2 v}{\partial z^2} \tag{2}$$

z-momentum:

$$0 = -\frac{\partial p}{\partial z} - \rho g \tag{3}$$

continuity:

$$\frac{\partial u}{\partial x} + \frac{\partial v}{\partial y} + \frac{\partial w}{\partial z} = 0 \tag{4}$$

density:

$$\frac{\partial \rho}{\partial t} + u\frac{\partial \rho}{\partial x} + v\frac{\partial \rho}{\partial y} + w\frac{\partial \rho}{\partial z} = \kappa\frac{\partial^2 \rho}{\partial z^2} \tag{5}$$

where f=2$\Omega$ sin$\phi$ and $\rho_0$,g,$\nu$,and $\kappa$ are constants. These five equations for the five variables u,v,w,p, and $\rho$ form the basis of geophysical fluid dynamics.

For our specific purpose in explaining the POP-model some more detail have to be included. Ocean dynamics are in this case described by the 3-D primitive equations.
*momentum equations*:

$$\frac{\partial u}{\partial t} + \mathbf{L}(u) - (uv\tan\phi)/a - fv = -\frac{1}{\rho_0 a\cos\phi}\frac{\partial p}{\partial \lambda} + \mathbf{F}_{Hx}(u,v) + \mathbf{F}_V(u) \tag{6}$$

$$\frac{\partial v}{\partial t} + \mathbf{L}(v) + (u^2\tan\phi)/a + fu = -\frac{1}{\rho_0 a}\frac{\partial p}{\partial \phi} + \mathbf{F}_{Hy}(u,v) + \mathbf{F}_V(v) \tag{7}$$

$$\mathbf{L}(\alpha) = \frac{1}{a\cos\phi}\left[\frac{\partial}{\partial\lambda}(u\alpha) + \frac{\partial}{\partial\phi}(\cos\phi\, v\alpha)\right] + \frac{\partial}{\partial z}(w\alpha) \tag{8}$$

$$\mathbf{F}_{Hx}(u,v) = A_M\left\{\nabla^2 u + u(1 - \tan^2\phi)/a^2 - \frac{2\sin\phi}{a^2\cos^2\phi}\frac{\partial v}{\partial\lambda}\right\} \tag{9}$$

$$\mathbf{F}_{Hy}(u,v) = A_M\left\{\nabla^2 v + v(1 - \tan^2\phi)/a^2 + \frac{2\sin\phi}{a^2\cos^2\phi}\frac{\partial u}{\partial\lambda}\right\} \tag{10}$$

$$\nabla^2\alpha = \frac{1}{a^2\cos^2\phi}\frac{\partial^2\alpha}{\partial\lambda^2} + \frac{1}{a^2\cos\phi}\frac{\partial}{\partial\phi}\left(\cos\phi\frac{\partial\alpha}{\partial\phi}\right) \tag{11}$$

$$\mathbf{F}_V(\alpha) = \frac{\partial\mu}{\partial z}\frac{\partial\alpha}{\partial z} \tag{12}$$

*continuity equation*:

$$\mathbf{L}(1) = 0 \tag{13}$$

*hydrostatic equation*:

$$\frac{\partial p}{\partial z} = -\rho g \tag{14}$$

*equation of state*:

$$\rho \;=\; \rho\,(\,\Theta, S, p\,) \;\rightarrow\; \rho\,(\,\Theta, S, z\,) \tag{15}$$

*tracer transport*:

$$\frac{\partial \varphi}{\partial t} \;+\; \mathbf{L}(\varphi) \;=\; \mathbf{D}_H(\varphi) \;+\; \mathbf{D}_V(\varphi) \tag{16}$$

$$\mathbf{D}_H(\varphi) \;=\; A_H\,\nabla^2\,\varphi \tag{17}$$

$$\mathbf{D}_V(\varphi) \;=\; \frac{\partial \kappa}{\partial z}\,\frac{\partial \varphi}{\partial z} \tag{18}$$

Here $\lambda$, $\phi$, z=r-a are longitude, latitude, and depth relative to mean level. $\rho_0$ is the reference density for sea-water and $f \;=\; 2\Omega\, sin\,\phi$ is the the Coriolis parameter.
The variables assumes always moving east for longitude and for velocity (u,v) west and north. In (16) $\varphi$ represents $\Theta$, S or a passive tracer. The pressure dependence of the equation of state is usually approximated to a function of depth. $A_H$ and $A_M$ are the coefficients (here assumed to be constant) for horizontal diffusion and viscosity, $\kappa$ and $\mu$ are the corresponding vertical mixing coefficients which typically depend on the local Richardson number. The third terms in (6), (7) are metric terms due to the convective derivatives in $d\mathbf{u}/dt$ acting on the unit vectors in the $\lambda$, $\phi$ directions, and the second and third terms in the brackets in (9),(10) ensure that no stresses are generated due to solid-body rotation. The forcing terms due to wind stress and heat and fresh water fluxes are applied as surface boundary conditions to the friction and diffusive terms $\mathbf{F}_V$ and $\mathbf{D}_V$. The bottom and lateral boundary conditions applied in POP (and most other Bryan-Cox models), are no-flux for tracers (zero tracer gradient normal to boundaries), and no-slip for velocities (both components of velocity zero on bottom and lateral boundaries).
*Spatial Definitions*
The location of model variables on the horizontal B-grid are, scalar at cell centres and vectors at cell corners. Scalars (T,S,p,$\rho$) are located at 'T-points' at the centres of T-cells, and horizontal vectors ($u_x$,$v_x$) are located at 'U-points' at the corners of the T-cells. The indexing for points (i,j) in the

logically-rectangular 2-D horizontal grid is such that *i* increases in the x-direction (eastward for spherical polar coordinates), and *j* increases in the y-direction (northward for spherical polar coordinates). A U-point with logical indices (i,j) lies to the upper right ($\sim$ northeast) of the T-point with same indices. The index for the vertical dimension *k* increases with depth, although the vertical coordinate z, measured from the mean surface level z=0, decreases with depth.
When the horizontal grid is generated, the latitude and longitude for each U-point and the distances HTN and HTE along the coordinates between adjacent U-points are first constructed. Then the latitude and longitude of T-points are computed as straight average of the latitude and longitude of the four surrounding U-points, and the along-coordinate distances HUW (HUS) between the adjacent T-points are computed as the straight average of the four surrounding values of HTE (HTN). Thus T-points are located exactly in the middle of the T-cell, but because the grid spacing in either direction might be non-uniform, the U-points are not located exactly in the middle of the U-cell.
In addition to the grid spacings HTN, HTE, HUS, HUW, several other lengths and areas are also used in the code. These can be defined as follows.

$$
\begin{aligned}
DXU_{i,j} &= 0.5[HTN_{i,j} + HTN_{i+1,j}] \\
DYU_{i,j} &= 0.5[HTE_{i,j} + HTE_{i,j+1}] \\
DXT_{i,j} &= 0.5[HTN_{i,j} + HTN_{i,j-1}] \\
DYT_{i,j} &= 0.5[HTE_{i,j} + HTE_{i-1,j}] \\
UAREA_{i,j} &= DXU_{i,j}DYU_{i,j} \\
TAREA_{i,j} &= DXT_{i,j}DYT_{i,j}
\end{aligned}
$$

DXU and DYU are the grid lengths centred on U-points, which DXT and DYT are those centred on the T-points. TAREA and UAREA are horizontal areas of the T-cell and U-cell, respectively.
The fields ULAT, ULONG, and ANGLE, are primarily used to interpolate the wind stress fields from a latitude-longitude grid to the model grid if needed. ULAT is used to compute the Coriolis parameter f at each model grid point.
*The Treatment of Time Steps*
Since POP is a z-level model, the depth of each point (i,j,k) is independent of its horizontal location. It is further divided up in 33 vertical levels.

The POP model uses 3-time step level second order accurate modified leapfrog scheme for stepping forward in time. As known a leapfrog scheme is typically used, when solving numerical problems concerning advection. It is here modified in the sense that some terms are evaluated semi-implicitly, and of the terms that are treated explicitly, only the advection operators are actually evaluated at the central time level, as the pure leapfrog scheme. In order to simplify further discussions a leapfrog scheme is included:

$$\theta_j^{n+1} \;=\; \theta_j^n \;-\; u\,\frac{\Delta t}{2\,\Delta x}\,(\,\theta_{j+1}^n \;-\; \theta_{j-1}^n\,) \tag{19}$$

A scheme that has the time step (n+1) on the left hand side, while time steps of (n, n-1) on the right hand side are called explicit. If the right hand side also includes a step of (n+1) it is referred to as implicit. On the other hand if the scheme includes both setups, it is called semi-implicit.
Leapfrog schemes can develop numerical noise due to the partial decoupling of even and odd time steps. In a pure leapfrog scheme they are completely decoupled and the solutions on the even and odd steps can evolve independently, leading to $2\,\Delta t$ oscillations in time. There are several methods to damp the leapfrog computational mode, two of which are currently implemented in POP. One is to occasionally take a forward step or an Euler forward-backward step (sometimes called a 'Matsuno' time step, Haltiner and Williams, 1980). The Matsuno step is more expensive than a forward step, but is stable to advection. The other method is to occasionally perform an averaging of the solution at three successive time levels to the two intermediate times, backup half a time step and then proceed. The later procedure is referred an 'averaging time step' (Dukowicz and Smith, 1994) and is the recommended method for eliminating the leapfrog computational mode. The advantage of the averaging step is that it places the solution on the average trajectory, whereas the forward and Matsuno steps select only one trajectory, corresponding to either the even or odd solution. Experience has shown that some model configurations are not stable using Matsuno filtering time steps, and this is especially true with the variable-thickness surface layer. The Matsuno step is a forward predictor step followed by a 'backward' step which is essentially a repeat of the forward step but using the predicted prognostic variables from the first pass to evaluate all terms expect the time-tendency term. On the very first time step of a spinup from rest a forward step is taken to avoid immediately exciting a leapfrog computational mode (this feature is hard-coded).

### 5.2 Ncl

CCSM also comes with its own script language, which resembles Fortran 90 in structure. The source files are all in the netCDF format, apart from some created files that might be in ascii.
All the calculation have been done using this language.

# 6 Model results

In the following a number of calculations are made. With these calculations different diagrams, graphs etc have been created. The calculations could be divided into several groups. Within each group analysis and comparisons between observational data and the model will be done. If appropriate other model results might be reflected upon.
If the need should arise to include both references and possible graphs these will be included with proper explanations to ease the discussion.
Examples of 150 year mean, Levitus data, Anomalies of temperature for Levitus and POP, SST anomalies, SST and SSS, SST in boxes, and Volume and Heat transports are given in the following. Finally a balance calculation will be presented
It should be noted as regards to anomalies means are yearly and periods are every five years starting with year 2. This obviously does not apply to anomaly comparisons of Levitus and POP.

### 6.1 Transects of temperature and salinity (Lev/POP) at $25\,^{\circ}$N

Generally the temperature change little during the year at this latitude.At about $20\,^{\circ}$W one can notice the influence of the Canary current with colder temperature at about 200 meters.

As can be seen from temperature anomalies for Levitus (Fig 1) and POP (Fig 2) presented later, the model is 1-2 degrees warmer in the upper 1000 metres at this latitude. It can be noticed that this predominates on the middle and western or American side of the basin, but a bit less on the eastern side.
It is doubtful how substantial the temperature rise according to the model is, but it is certainly noticeable. The general consensus is that global warming is occurring, but that climate modelling still have a long way to go before this picture is complete. Atmosphere and ocean is not completely coupled as yet. Additionally chemical and biological parameters should be part of the equation before clear conclusions can be made.

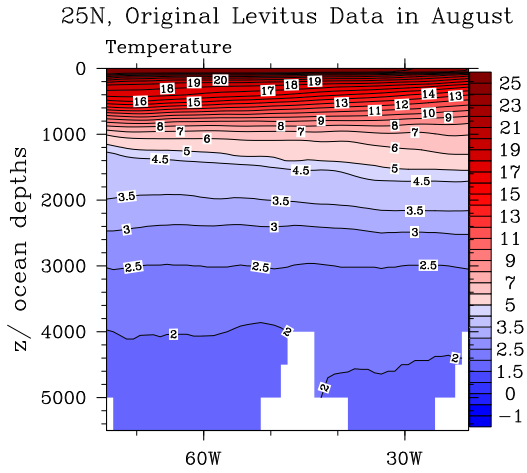


Figure 1: Temperatures at 25N (Levitus) in August

The mentioned trend showing a temperature increase continues down to about 1400 metres, after which will follow depth ranges that seem to show no difference in temperature between Levitus (Fig 1) and POP (Fig 2). At about 4000 metres the Levitus temperatures are 0.5 °C warmer than POP. The Levitus temperature seem to bend downward more due to the topography than the POP (Fig 2) temperatures. This could be because of compression. Also the isotherm of 1.5 °C for POP (Fig 2) seem more or less to travel straight through the topography, or at least more or less so. In addition the temperature of 2 °C seem more realistic at this depth.

There is also quite a few differences when it comes the salinity at this latitude, although the differences over the year are for both types of data small.

In the top 1000 metres the Levitus data (Fig 3) has more uniform structure, than the POP data (Fig 4). The POP values in this depth range is also a lot lower than for Levitus. There is an isohaline close to the surface at about 30 °W of 35.2, whereas the same area for Levitus displays a value of about 37. Lower values of 36.2 can also be shown in the middle of the ocean for POP at 500-600 metres, which is probably 0.5-0.8 lower than the Levitus series.

This an area of high evaporation, which will tend to increase the salinity. In order to reduce the salinity , freshwater needs to be added. This can be

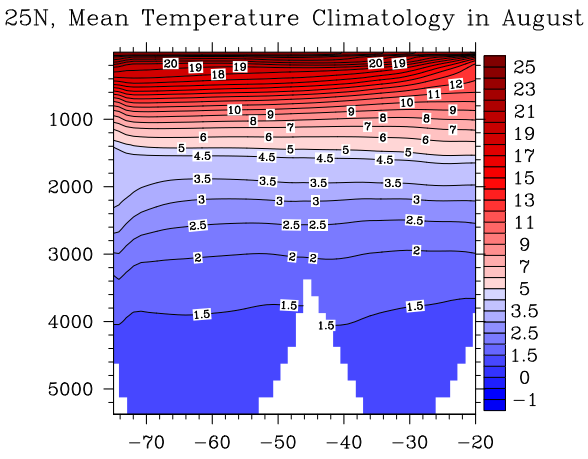


Figure 2: Temperatures at 25N (Pop) in August

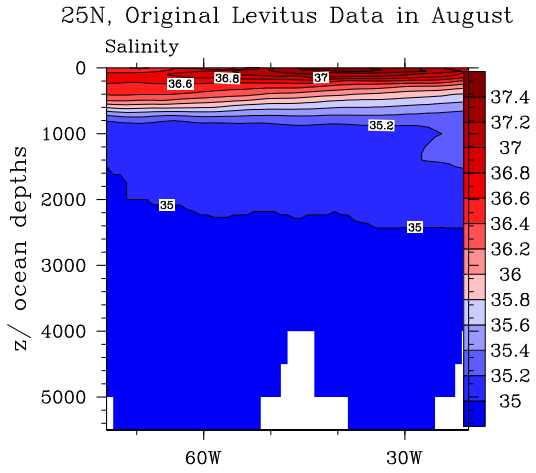


Figure 3: Salt at 25N (Levitus) in August

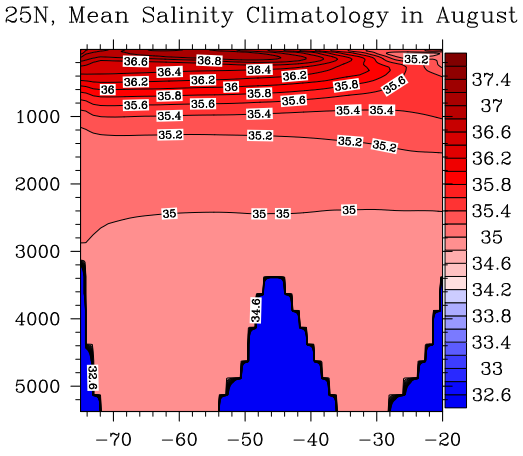


Figure 4: Salt at 25N (Pop) in August

done either with increased precipitation or runoff from rivers, or possibly both. The above mentioned isohaline of 35.2 can possibly be explained by river runoff, while a salinity value of around 36.2 is possibly due to precipitation.
It can be noticed that a lower isohaline of 35.2, which possibly is associated with an Atlantic water mass, is for the model located at about 1200 to 1300 metres, while for Levitus (Fig 3) it can be found at about 800 metres with a dip down to 1300 metres at 30 °W.
Atlantic water is defined as having a salinity of 35. This isohaline will for the Levitus (Fig 3) series be found from 1600 metres to 2200 metres, bending upwards at the western side. For the POP (Fig 4) model this isohaline can be found at a lower depth close to 3000 metres.

## 6.2 Transects of temperature and salinity (Lev/POP) at 45 °N

Looking at the transects at this latitude it should be noted that the coverage of the Levitus series and the model data are a bit different, so that only longitudes between 20 °W and 60 °W are shown for Levitus, while up to about 70 °W for POP. This is though enough in order to make the comparisons in question.

Also at this latitude there marked differences between Levitus (Fig 5)

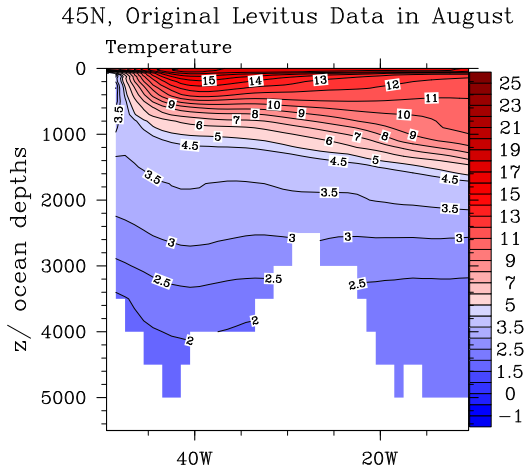


Figure 5: Temperatures at 45N (Levitus) in August

and the model. Closer to the surface there will be an increase of about 2 °C in the POP model (Fig 6) at 20 °W at about 400 metres. The difference can not be noted to the west of this longitude.

After that temperatures will not differ down to about 1000 metres. The middle will show a difference as compared to 25 °N latitude. The 4.5 °C isotherm is for Levitus (Fig 5) located at around 1000 to 1200 metres, while for POP (Fig 6) 1600 to 1800 metres, bending in different directions at 20 °W. Also the 3.5 °C isotherm lies lower for POP (Fig 6) than Levitus (Fig 5) and can located be at 2000 to 2600 metres compared with 1600 to 2000 metres. Again the isotherm bends down to its largest depth for POP (Fig 6) on the western side of the diagram, for Levitus (Fig 5) it is the other way around.

Moving down to 4000 metres the same difference of 0.5 °C can also be noted at this latitude.

As was mentioned at a latitude of 25 °N the temperature is higher closer to the surface according to the model. If this fair, later discussions will reveal.

In regards to salinity there are small differences over the year, although it is the data material of the two series that should be investigated. On the other hand when comparing the material there are some differences.

Close to surface (around 400 metres), and investigating at 30 °W, POP

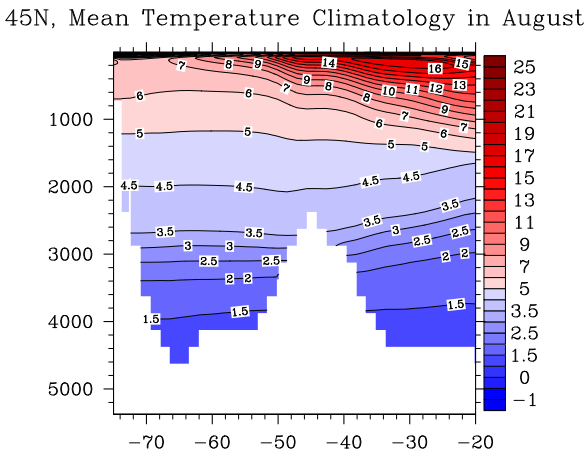


Figure 6: Temperatures at 45N (Pop) in August

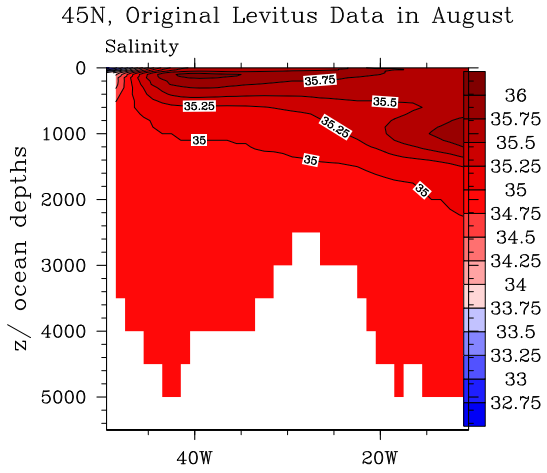


Figure 7: Salt at 45N (Levitus) in August

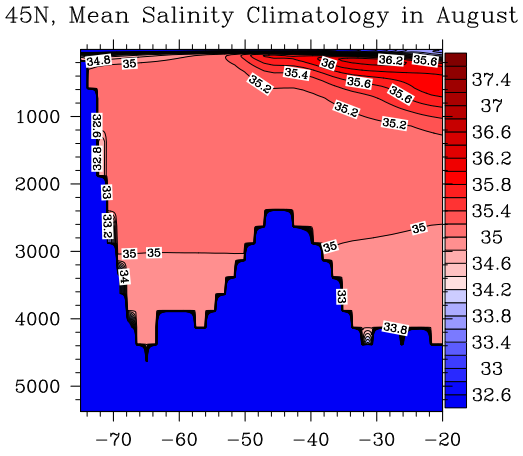


Figure 8: Salt at 45N (Pop) in August

(Fig 8) will have a value of 36 while for Levitus (Fig 7) the isohaline of 35.5 will be located at this depth.
The difference of the 35 isohaline is more marked. For it is located at a depth of about 3000 metres for POP (Fig 8), while for other series it can be found down to 2200 metres bending up close to the surface on the western side. It should be commented upon that while isohaline for Levitus (Fig 7) is only one connected all the way, for POP (Fig 8) it is one at depth and a small one closer to the surface. The reason for this could be due to the fact the two diagrams have different extensions on the western side, although it goes deeper for the POP material.

## 6.3 Transects of temperature and salinity (Lev/POP) at 60 °N

At this latitude there are also substantial differences. Earlier it has been mentioned that model might be too warm at this latitude, but by how much is difficult to say. The analysis will be performed as normal regardless of this.

The temperature will vary a bit at the surface at this latitude, but not with much. So it is quite appropriate to use the January transects for comparison. As before a comparison is made at 400 metres and 30 °W, when considering the top 1000 metres. There is a substantial increase of the tem-

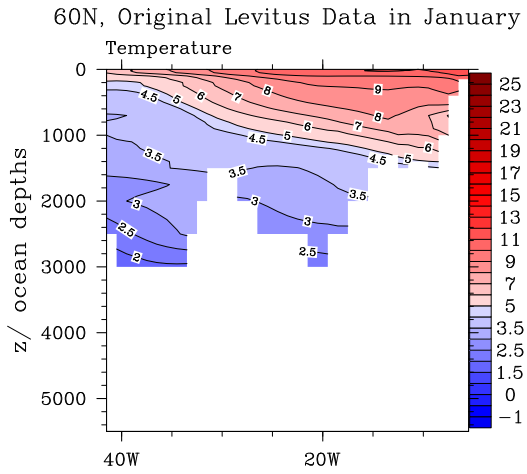


Figure 9: Temperature at 60N (Levitus) in January

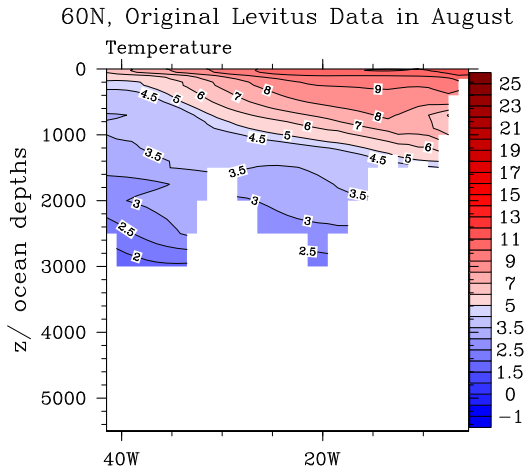


Figure 10: Temperature at 60N (Levitus) in August

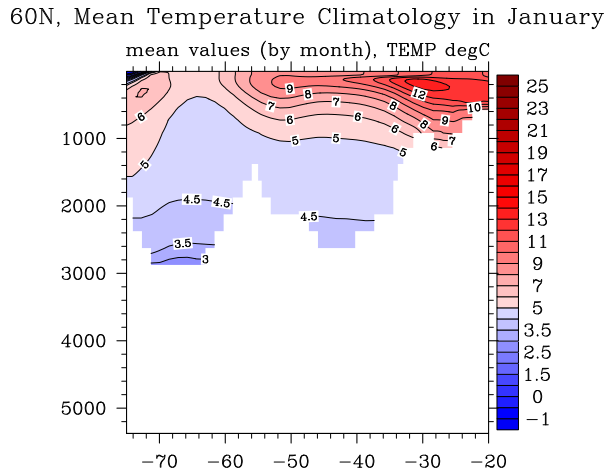


Figure 11: Temperature at 60N (Pop) in January

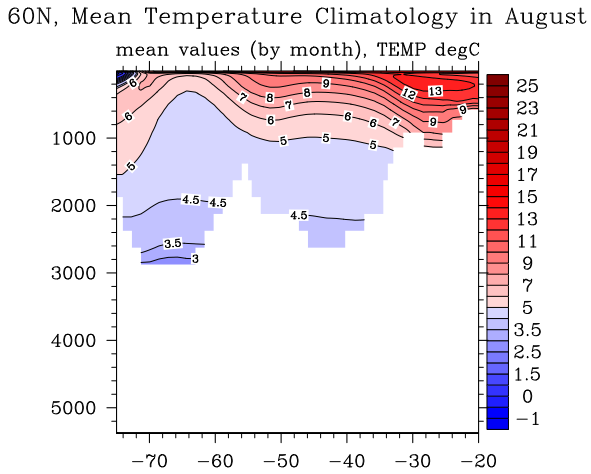


Figure 12: Temperature at 60N (Pop) in August

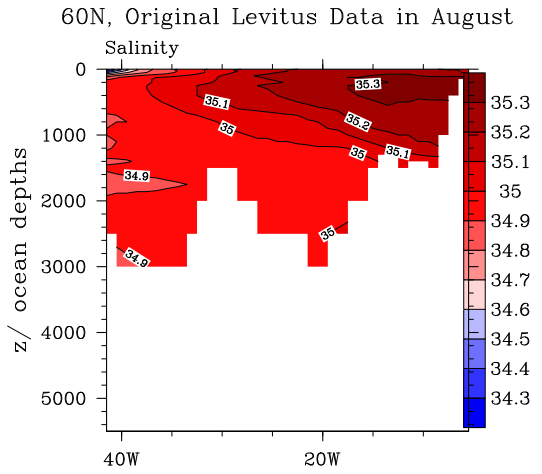


Figure 13: Salt at 60N (Levitus) in August

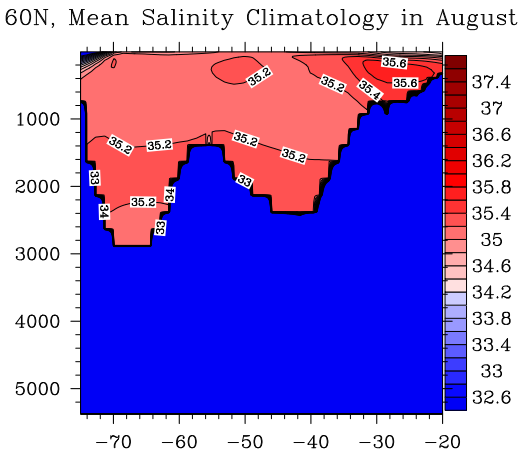


Figure 14: Salt at 60N (Pop) in August

perature with 4 °C at this depth.
Even if we cut this temperature rise in half it is still substantial. It is not completely out of character to say that there is a trend, at least east of 30 °W, of a general temperature rise in the upper layers of the ocean according to the model.
Additionally at 40 °W it can be seen that the 4.5 °C isotherm cuts deeper for POP (Fig 11 and 12) than Levitus (Figures 9 and 10), 1800 to 200 metres, respectively, which certainly is substantial difference.
Looking at salinity the structure difference is smaller. Again comparing 30 °W and 400 metres the POP (Fig 14) model displays 35.6 while Levitus (Fig 13) displays 35.1.
The 35 isohaline can be seen for Levitus, while it seems difficult pin point for the POP model, but can be seen as a large area from 200 to 1200 metres. But for Levitus this isohaline travels from the surface around 35 °W to 1000 metres at 20 °W. The conclusion must be that for a salinity of 35 (Atlantic water) there is no marked difference between Levitus and POP.

## 6.4 Transects of temperature and salinity (Lev/POP) at 30 °W

These diagrams follow a longitude of 30 °W with the y-axis showing depth and northern latitude up 40 °N as the x-axis. Small differences over the year can be noticed, which should not be surprising in reference to earlier discussions.

Investigating at 30 °N and around 400 metres of depth the POP model (Fig 16) is as expected 2 °C warmer. Moving down to 1000 metres the difference is only 1 °C.
Below 1000 meters the different isotherms will vary according to Levitus (Fig 15) and POP (Fig 16). The 4.5 °C isotherm will located at about 1500 metres for POP, but the same isotherm will located at 1300 metres for Levitus.
With the isotherm 3.5 °C having about the same location for both the series, below 2000 metres the difference will revers itself, until, as has been discussed earlier, Levitus is 0.5 °C higher at 4000 metres.
From a salinity point of view there are small differences between the data series. At about 40 °N the influence from the Mediterranean can be seen. The 35 isohaline is nicely developed in Levitus, but the message is the same and covering the same depths (Figures 17 and 18).

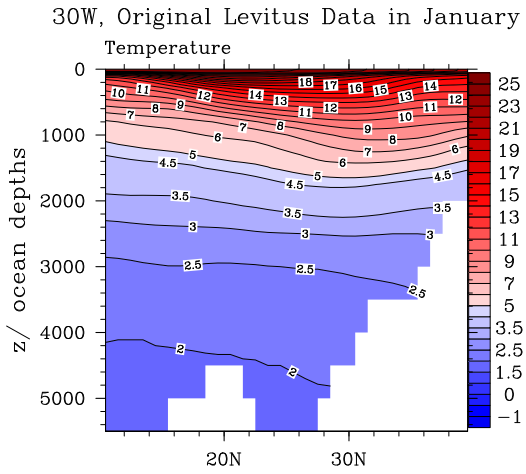


Figure 15: Temperature at 30W (Levitus) in January

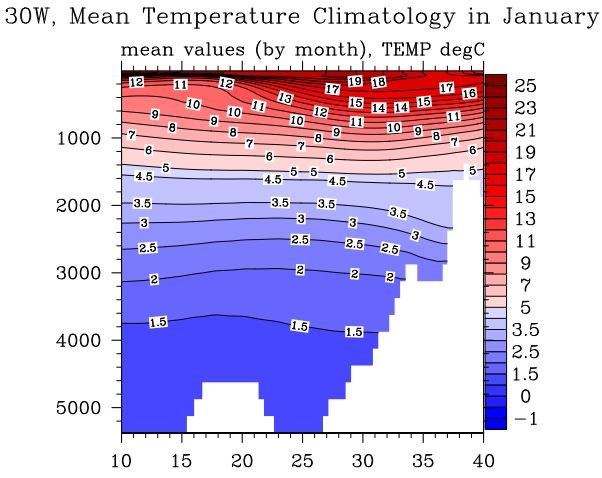


Figure 16: Temperature at 30W (Pop) in January

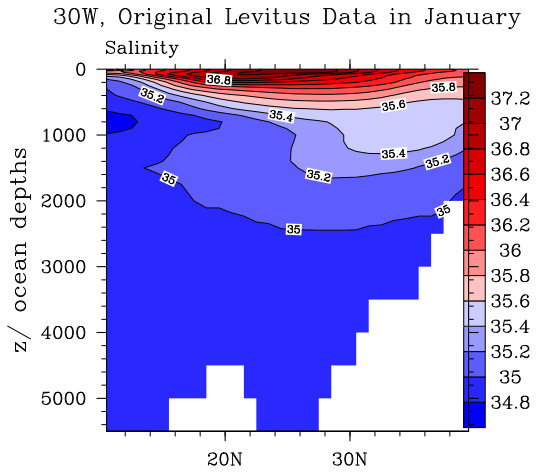


Figure 17: Salt at 30W (Levitus) in January

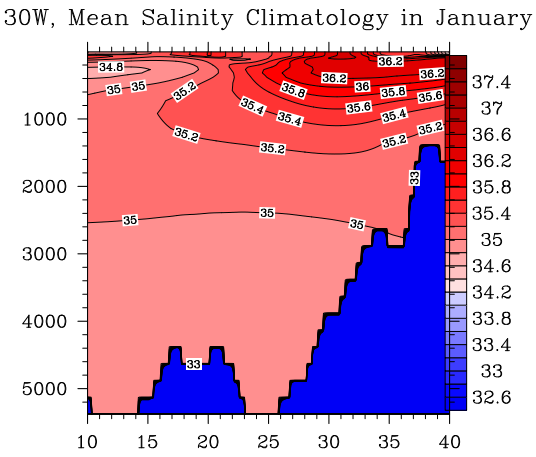


Figure 18: Salt at 30W (Pop) in January

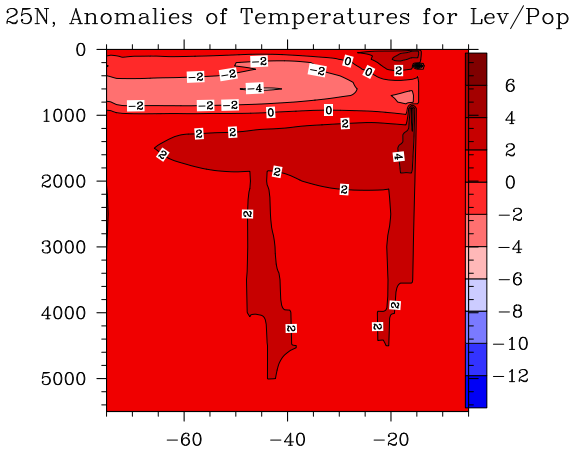


Figure 19: Anomalies Lev/POP at 25N

## 6.5 Anomalies for temperature Lev/POP

These few diagrams tries to compare the difference in temperatures as provided by Levitus to those provided by POP. Mean values have been calculated in both cases and POP values have been deducted from Levitus values. Although these have been called anomalies they are strictly speaking means ddeducted from means, but with the absence of a better word anomalies have been used.
A negative value would therefore mean that the model has simulated a larger positive or negative value than Levitus. Only positive values could obviously be assumed as a mean of negative values would impossible for latitudes between the Equator and 60 °N.

### 6.5.1 Values at 25 °N

At this latitude (Fig 19) there are quite a number of differences. Down to about 1000 meters anomalies between $-2$ °C and 2 °C will occur, with a maximum of $-4$ °C. This means that the model on average is that much warmer or colder in this area as explained above.

A value of $-2$ °C will occur at between 25 °W to 80 °W. The latter longitude being in the Gulf Stream belt. This means that more heat is being

transported in *the Stream* than before. An even higher decrease of $-4\,^{\circ}$C can be noticed at 600 metres between 40 °W and 50 °W. Closer to the coast of Africa there is a increase or status quo in the anomalies nearer the surface between 20 °W and 30 °W, which means that the Levitus temperatures are higher than POP temperatures.
In the deeper ocean the situation is quite different and the values are reversed. A broad belt from 1200 to 1800 metres and from 15 °W to 60 °W with anomalies of 2 °C, and even a small patch of 4 °C in the most eastern extension of this area. At points of 20 °W and 45 °W tongues of these characteristics reach down close to 5000 metres. The conclusion being that Levitus has higher values than POP.

### 6.5.2 Values at 45 °N

Here in the mid-latitudes (Fig 20) the picture can be said to be even more complex.
Starting the investigation again above 1000 metres. It can be seen that down to 600 metres, the POP model has a lot higher temperatures from just outside the African coast to around 45 °W. Again anomalies of $-2\,^{\circ}$C, or even $-4\,^{\circ}$C, can be seen. The lowest anomalies (highest POP temperatures) in a band from 15 °W to 30 °W.
Moving west of this area the values for the anomalies have been changed with the same magnitude, but now being positive instead of negative. The longitude band in question now being 45 °W to 65 °W, with the same depth range. At about 70 °W there is a band of an anomaly of $-2\,^{\circ}$C to complicate the picture.
Moving down in depth positive or unchanged anomalies completely dominates the area under investigation, which means that the POP temperatures are lower than the Levitus temperatures. The highest anomalies are found closer to the eastern part (10 °W) at 1000 metres.

### 6.5.3 Values at 60 °N

As has been mentioned earlier the model is too warm at this latitude (Fig 21), but as it is difficult to know with how much any reflections to this fact can be ignored, as the analysis will be done with what is available. Reflections of this fact will though be discussed inside topics concerning the *Model* and within the *Conclusions*.

Glancing quickly at the values at this latitude, the anomaly variations appear to be a bit more structured, layered (stratified) it would appear. Further analysis will reveal if this is the case.

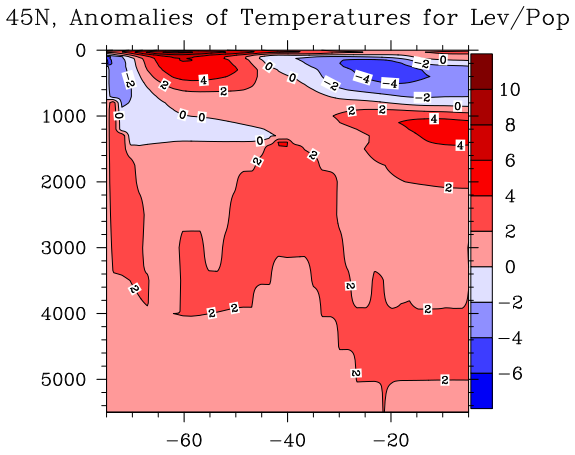


Figure 20: Anomalies Lev/POP at 45N

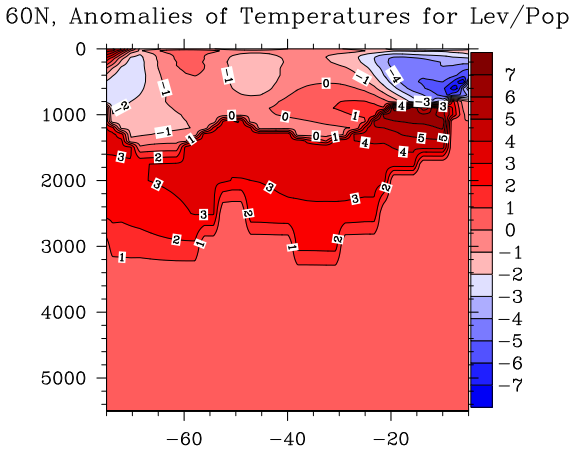


Figure 21: Anomalies Lev/POP at 60N

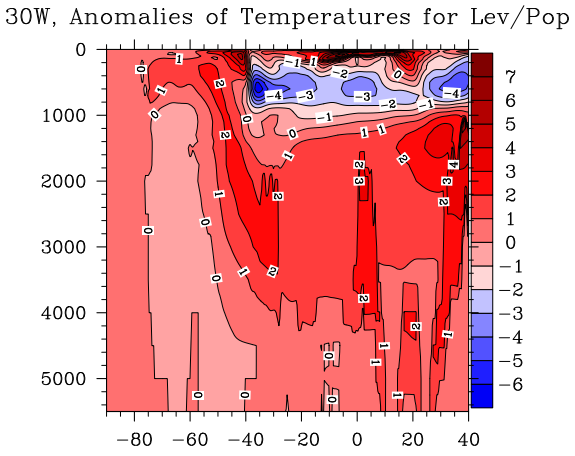


Figure 22: Anomalies Lev/POP at 30W

Above 1000 metres most anomalies appear to vary between $-1\,^{\circ}$C and $-4\,^{\circ}$C, with the lowest values in the eastern part of the diagram (10 °W to 20 °W) and down to 800 metres. There are some exceptions however, but the earlier statement is at least true down to 800 metres. Even extreme negative values close to $-7\,^{\circ}$C can be seen at 5 °W and 600-800 metres.
Below 1000 metres the temperature anomalies varies between $0\,^{\circ}$C and $5\,^{\circ}$C, with the highest values at 1200 metres and from 5 °W to 25 °W.
As has been mentioned in the preceding section, POP has higher values above 1000 metres and lower values below 1000 metres.

The difference at this latitude is in places extremely high, so both a closer search into other material pertaining to this latitude need to be made.

### 6.5.4 Values at 30W

Here the transect (Fig 22) is along a number of latitudes, with the depth ranges being from the surface to the bottom. The latitudes shown in the figure are from 80 °S to 40 °N. Only the northern latitudes will be analysed here.
Above 1000 metres both neutral, positive, and negative values can be seen. It is though quite clear that the negative values dominates, with the lowest values (highest POP temperatures) towards the most northern latitude,

being 30 °N. The same trend as before can be seen with the POP temperatures showing a temperature increase of 4 °C. Without preaching about global warming, that a lot of scientists claim is happening, it shows as has been seen earlier as well a clear trend that the temperatures in the coming 150 years (or from about 1990) according to the model are increasing.
Below 1000 metres there are only positive anomalies, with the highest toward the northern end and at about 1600 metres.

## 6.6 Temperature Anomalies

This part will include a number of temperature anomalies at 25 °N, 45 °N, and 60 °N for the modelled years 2, 12, and 22, which covers about the same range of years as the SST anomalies in the following section.
This has been done in order to show a more complete pattern of possible trends in regards to changes.
Anomalies of $\pm 0.1$ °C are considered to be large. In this material we can see that in places the anomalies are a lot greater.
Our main objective to changes of the transport of heat from the western boundary current (*id est* Gulf Stream) onto the North Atlantic Current and its further circulation towards northern Europe and southern Europe and northern Africa.

### 6.6.1 Anomalies at 25 °N

This latitude, which is within the subtropical gyre show anomlies that are equal or greater to $\pm 0.1$ °C in parts of the basin within the observed time periods.
As can be seen the anomalies (Figures 23,24, and 25) are at their greatest close to the surface, and also close to the coasts of Africa and Latin America. The edges are of course the areas of western and easter boundary currents. The former should be warmer and the latter should be colder. For most part the western side show negative values up to $-0.2$ °C, while the eastern side display positive values up to 0.2 °C. This means that the 150 year mean is higher as compared with the western side, but lower as compared with the eastern side.
What could said is that the anomalies are substantial in the surface region, and that external influences certainly are present.

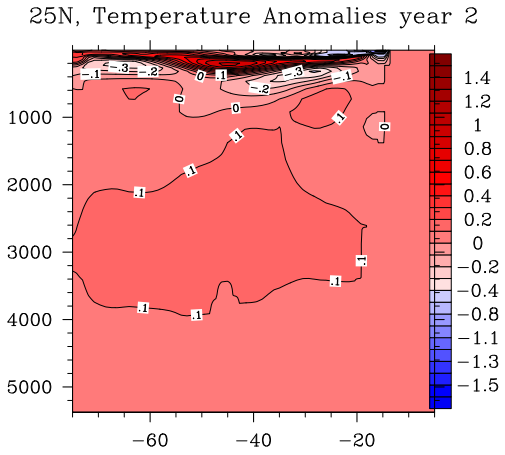


Figure 23: Anomalies for year 2 at 25N

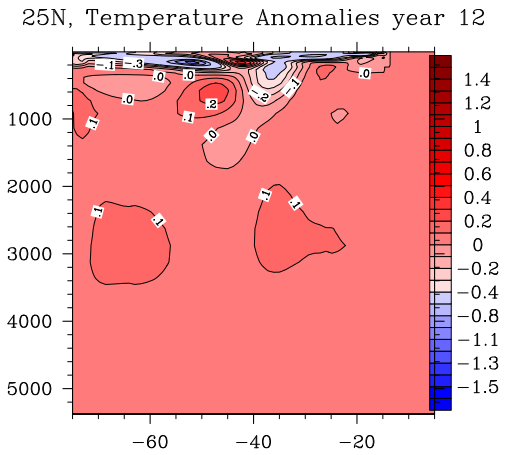


Figure 24: Anomalies for year 12 at 25N

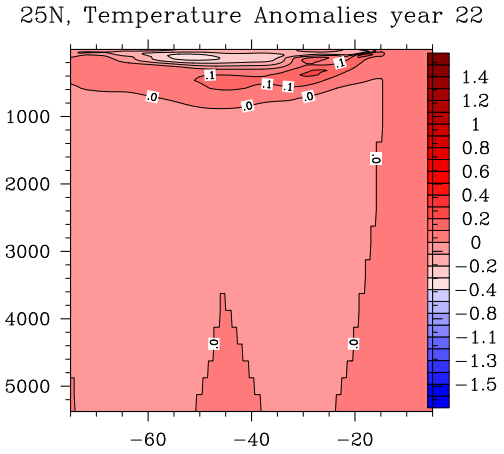


Figure 25: Anomalies for year 22 at 25N

### 6.6.2 Anomalies at 45 °N

At this latitude (Figures 26,27, and 28), which is in the belt where the *Gulf Stream* continues into the *North Atlantic Current* the anomalies doubles and even trebles in the surface layer.
Here negative values are spreading from 70 °W to 30 °W with anomalies of $-0.4$ °C, for year 2. These will be reduced substantially as one moves close to the African coast. The observations for year 12 change somewhat. The same negative value of $-0.4$ °C can be seen from 70 °W to 55 °W, while in the middle of the ocean from 55 °W to 30 °W this year show positive anomalies up to 0.5 °C, these are also penetrating quite deep (1000 metres). Moving on to year 22 the pattern has been reversed once again. This time the anomalies are even greater. To a depth of 300 metres from 70 °W to 45 °W one can see anomalies up to $-0.9$ °C, which are extremely high. Also in the surface area closer to the African coast quite low values can be seen. On the eastern though an anomaly of 0.2 °C at 1000 metres (20 °W) can be seen.
The point here is that it takes 10 years between these extremes. What external and internal factors that contributes to these kind of fluctuations are quite difficult know at present, and is certainly open for debate. A lot of parameters are still missing when simulating these kind of conditions. But

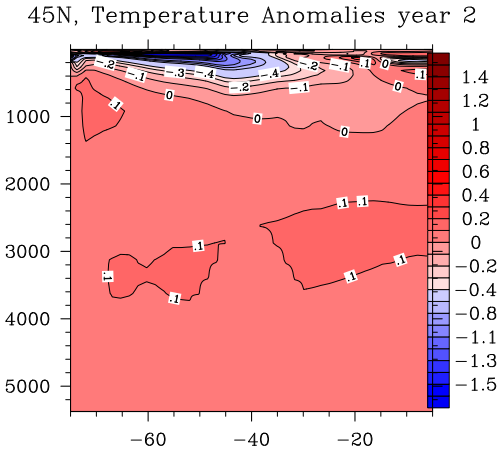


Figure 26: Anomalies for year 2 at 45N

it seems fair to say that it certainly should be investigated further.

### 6.6.3 Anomalies at 60 °N

At this high latitude (Figures 29,30, and 31) we also find large anomaly variations. Although these are a lot smaller than at 45 °N. Also here the anomalies are largest close to the surface, which seems to indicate the influence of surface currents. They are located primarily between 40 °W and 20 °W, which is where the North Atlantic Current is split into a northward and a southward part. Fluctuations between −0.3 °C and 0.1 °C can be seen in this area. Further east even greater fluctuations can be seen (−0.7 °C to 0.5 °C ). Also west of 40 °W the same trends can be spotted. It should though be noticed that during years of an negative anomaly on the western side a positive anomaly is displayed on the eastern side, and vice versa.
As is being remarked upon in several sections in this document, the model is too warm at 60 °N. It is though quite clear that also here the anomalies are substantial.

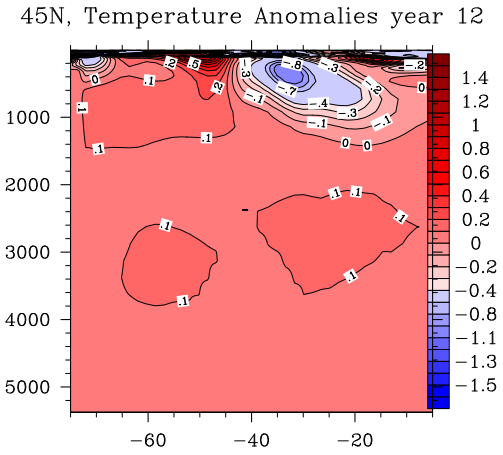


Figure 27: Anomalies for year 12 at 45N

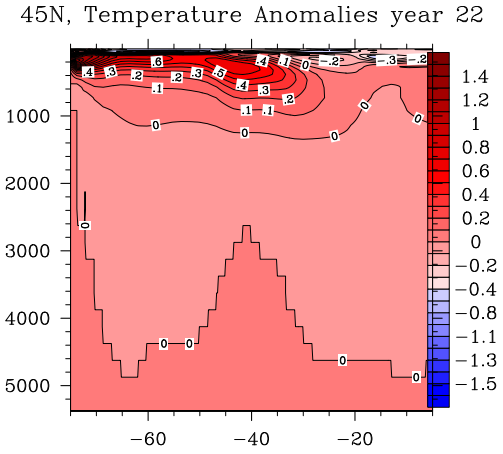


Figure 28: Anomalies for year 22 at 45N

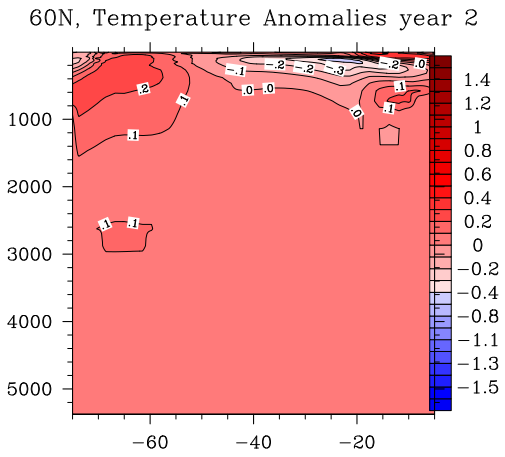


Figure 29: Anomalies for year 2 at 60N

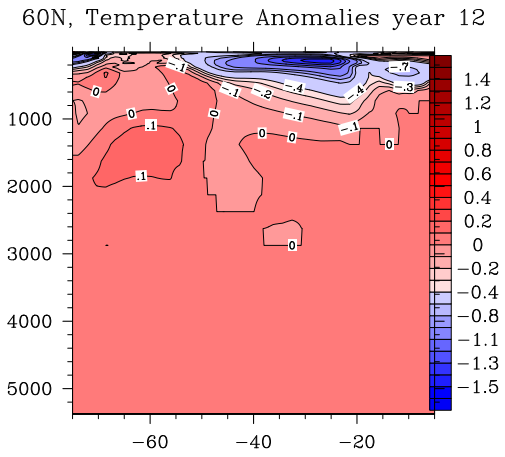


Figure 30: Anomalies for year 12 at 60N

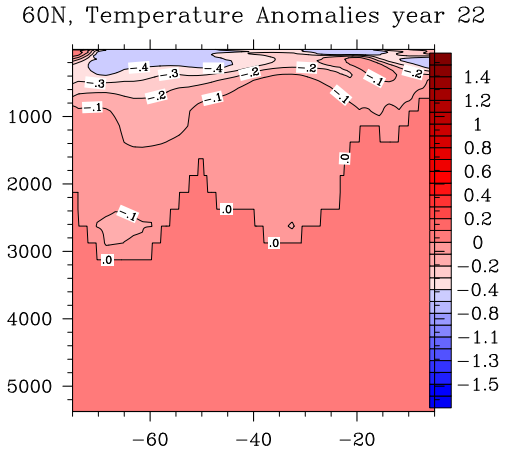


Figure 31: Anomalies for year 22 at 60N

## 6.7 SST Anomalies

You can observe temperature anomalies being transported from the Pacific Ocean to the Norwegian Sea. The duration of this is about 25 years.
Anomalies will be investigated from the equator to about 60 °N.
The material will cover the first 25 years, which will agree reasonably well with the period of time that the temperature anomalies are covering.
Our aim is to investigate the area, where the subtropical gyre is active. The question is how surface temperature will change, and hence heat, over the modelled period, in the area in question (Figures 32 through 39 should be consulted).
The total mean of SST anomalies have been calculated by deducting the total mean over 150 years from the five year mean in question.
Anomalies of $\pm 0.1$ °C can be considered to be relatively substantial. As can be seen the anomalies are lot greater than this.
One would expect high surface temperatures in the equatorial area, due to the high solar insulation. At about 25 °N the temperature should be higher on the western side than on the eastern side. The reason for this is in the former case the western boundary current being warm, while in the latter case due to the cooler eastern boundary current and upwelling.
Moving on to 45 °N the SST should show a pattern of relatively warm

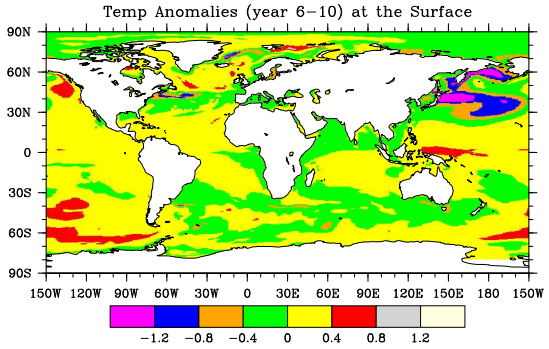


Figure 32: SST Anomalies year 6-10

temperatures during summer with the eastern side again having the lowest temperatures. During winter though at this latitude the situation reverses, so that the western side now has the lowest surface temperatures, while the the eastern side the highest.
At 60 °N the pattern is similar, although lower temperatures moves further east.

### 6.7.1 From Equator to 25 °N

The maximum anomaly is here between $-0.4$ °C and 0.4 °C. A negative value means that the 150 year mean is higher, while a positive value means a higher value of the 5 year period. It will take 1-2 periods to switch between the intervals. It is difficult to make too much out of these variations as they are located within an interval and it is not known how close they are to zero. But as could be seen in the section on temperature anomalies they certainly are substantial also in this area. It should be noted that after about 25 years an anomaly between 0.4 °C and 0.8 °C can be seen outside the coast of Africa, which shows a large increase in temperature for this period. This will occur within time periods of 25-30 years.

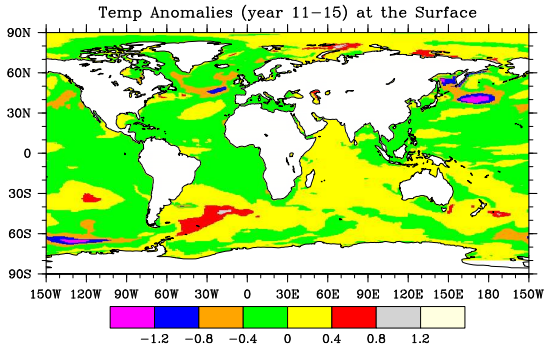


Figure 33: SST Anomalies year 11-15

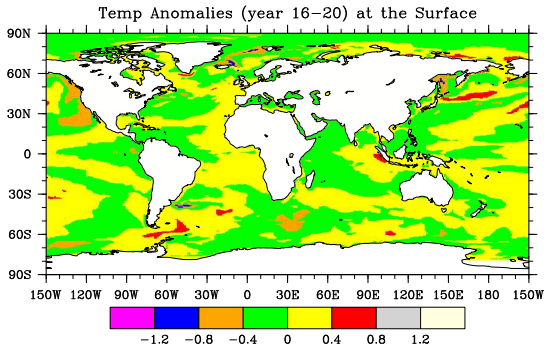


Figure 34: SST Anomalies year 16-20

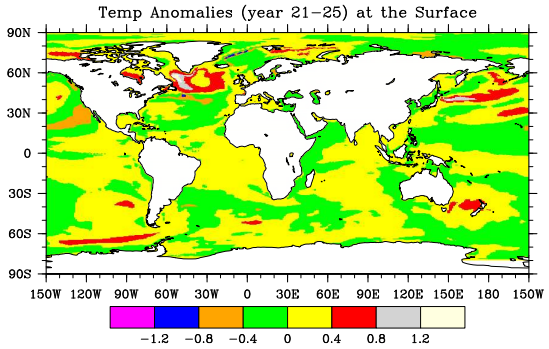


Figure 35: SST Anomalies year 21-25

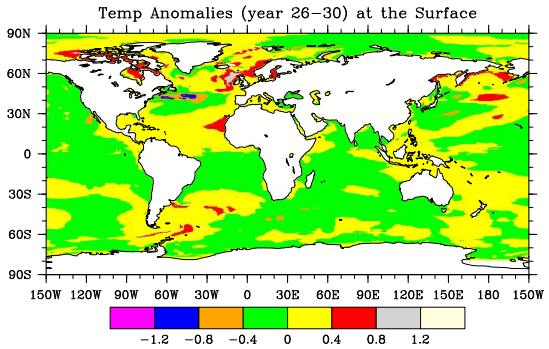


Figure 36: SST Anomalies year 26-30

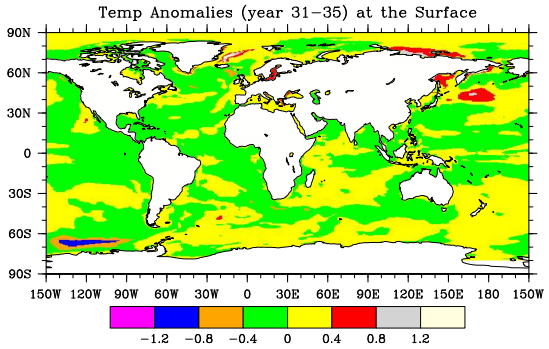


Figure 37: SST Anomalies year 31-35

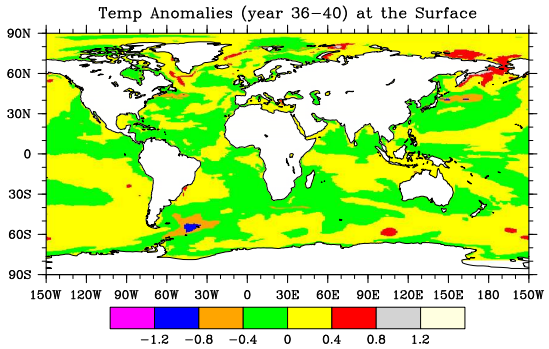


Figure 38: SST Anomalies year 36-40

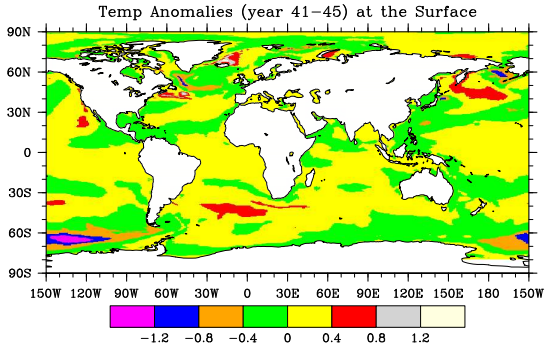


Figure 39: SST Anomalies year 41-45

### 6.7.2 30 °N to 60 °N

This is an area where the North Atlantic Current travels (or to a greater extent the Norwegian Current), so the variations over the periods are a lot more varied and substantially greater.
The *Gulf Stream* is swift and narrow and the *North Atlantic Current* is the continuation as it travels north and east. Having crossed the the Atlantic part of it flows north as the *Norwegian Current* and the other part flows south. The southward flowing part is lot slower broader and more diffuse, which the *Canary Current* is an example of, it will however feed into the *Gyre* in order to complete the loop.
Initially it should remembered that the model is quite a lot warmer in part of this area, than what have been observing, so analyses reflected upon in this document are obviously based on the simulated reality, that is displayed.
The transport of heat with the North Atlantic Current to the neighbourhood of Scotland seem to have a duration of about 20 years (four periods of five years). This is due to the fact that the simulation starts at year 6, although strictly speaking it starts on year 2, but year 3 is a bit patchy so it seems better to start with year 6. In order to complete a loop so that heat again flows in a substantial amount from Scotland to the Norwegian coast

will take 30 years according to the model.
In the middle of the ocean especially just below 60 °N the variations in this time frame varies from $-0.8$ °C to $-0.4$ °C on the lower range to 0.4 °C to 0.8 °C at the the higher end. This means that either the five year period shows warmer temperatures or it shows greater temperatures as compared to the 150 year mean. Temperature anomalies in the range of $\pm 0.4$ °C to $\pm 0.8$ °C are large, so suspicion regarding temperature changes in the ocean due to to external conditions are within a high probability.

## 6.8 Temperature and Salinity in global box

Observed values for mean temperature and salinity (Figures 40 and 41) for all oceans have been approximated to 3.5 and 34.7. As can be seen from these two plots that seem to fit quite well. From this it can be deduced that the model calculations arrive at reasonably correct values.

## 6.9 SST means for all oceans

This diagram is a mean (Fig 42) covering all oceans. Looking at the Atlantic from the Equator to 60 °N the following can be said.
At the equator the temperatures lie in the interval 25 °C to 28 °C, which is what you would expect.
Moving north to 25 °N the temperatures lie in the interval 20 °C to 25 °C with a small patch in the interval 25 °C to 28 °C at the American coast. This is also quite normal with higher values being located in the *Gulf Stream* belt.

Now investigating 45 °N the interval in question is 15 °C to 20 °C. Also these values is what could be expected.
The last latitude that are being investigating is 60 °N. Here the values are divivided up into three intervals. Towards Europe from 30 °W the values lie in the interval 10 °C to 15 °C, from 30 °W to 50 °W in the interval 5 °C to 10 °C, and to the west of this in the interval 0 °C to 5 °C. The values do seem to fit quite well, considering the knowledge of a bit warmer temperatures on the European side that the model is expected to return.

## 6.10 SSS means for all oceans

This diagram displays the mean (Fig 43) salinity covering the total 150 years for all oceans. For the Atlantic the values could be summarised as

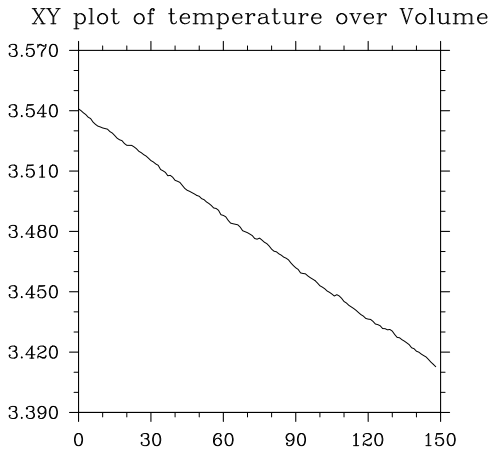


Figure 40: Average temperature over all basins

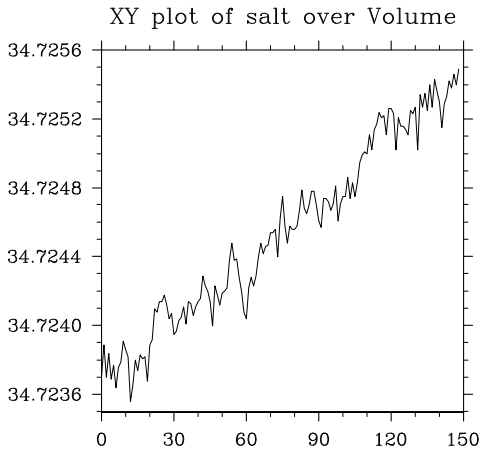


Figure 41: Average salt over all basins

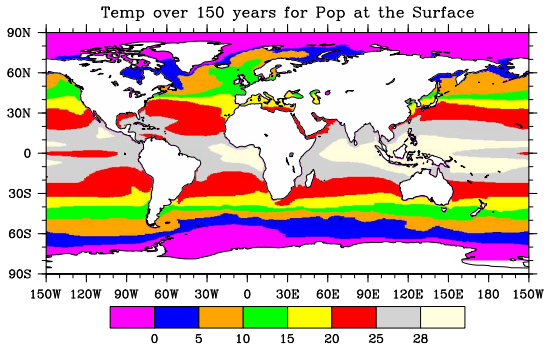


Figure 42: SST across all oceans

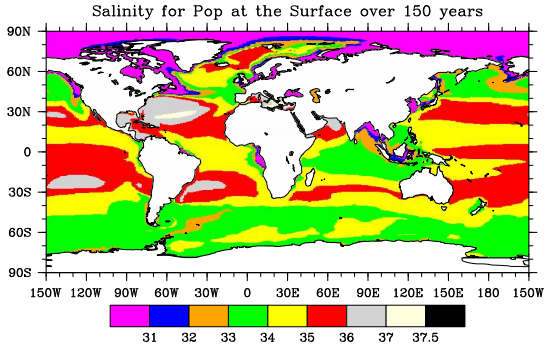


Figure 43: SSS across all oceans

follows:
At the equator the salinity lies in the interval 34 to 35, with lower values at the coasts due to river runoff, which is more marked at the African side. All of this is quite normal.
By travelling to 25 °N the salinity is bit more varied. From 30 °W to the American coast values will lie in the interval 36 to 37 (an enclosed area of 37 to 37.5 can be seen here). A thin band just east of 30 °W values of 35 to 36. Finally in the eastern part values between 34 and 35 could be noticed.
Studying the latitude 45 °N, four bands of salinities can be noticed. Starting from the west less than 31, 31 to 32, 32 to 33, and 33 to 34.
Finally winding up at 60 °N, it can be seen that at the coasts the salinity is around 31, while in the rest of the ocean in the interval 34 to 35. This would seem to be quite normal.

## 6.11 SST in Boxes

We have here from CCSM2 calculated SST in boxes from the Equator up to 60N in the North Atlantic. Three boxes have been made. The calculations are yearly means, covering the complete period of 150 years (Consult Figures 44 through 46).

In the box between the Equator and 25 °N latitude there are variations in temperatures between 25.3 and 26.2 °C, which seem to be quite normal for this area of the Atlantic. It can also be noted that a reduction in temperature up to 0.5 °C can be noticed as we are approaching the end of the simulation period.
The following box covers 25 °N to 45 °N of latitude. Here the variations are between 20.1 ° to 20.9 °C. This does not seem to be unreasonable, but rather quite normal. The values seem to fluctuate, but any clear trend of higher temperatures towards the end of the period cannot be noticed.

The last box of SST's is covering a latitude between 45 °N to 60 °N. Variations are here between 7.8 ° to 9.2 °C. This also seem to be quite a normal development. If for example a check is made on the available Levitus data over a year this range can be found. It should be noticed that the temperatures in the model are too high at about 60 °N, but this would be difficult to notice as temperatures have been averaged over years and that the model at 45 °N does not generate too high values.

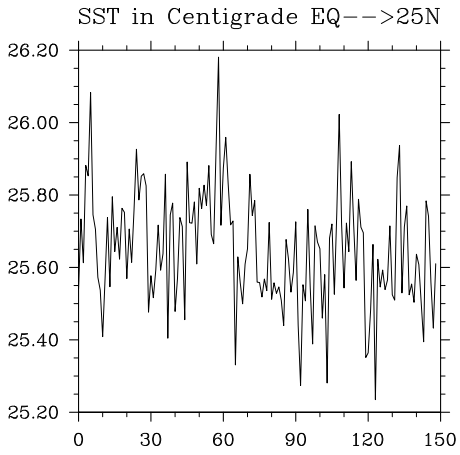


Figure 44: SST in box Equator to 25N

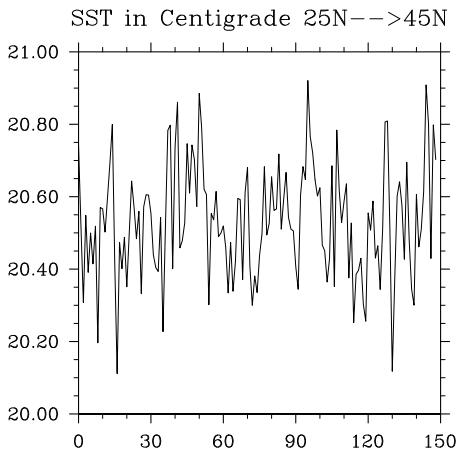


Figure 45: SST in box 25N to 45N

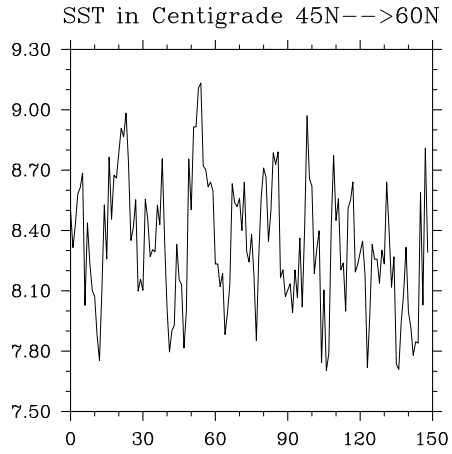


Figure 46: SST in box 45N to 60N

## 6.12 Calculations for Volume and Heat in the North Atlantic

Included are eight xy-plots for the volume and heat transports at the Equator, 25 °N, 45 °N, and 60 °N. The calculations are yearly means, covering the whole period of 150 years. The volume calculations are in Svedrups. while the heat transports are in PW.
In order to make some comparisons with observational data, as these are missing from the Levitus series, calculated values from WOCE (World Ocean Circulation Experiment) [1] have been chosen. They are available online, so those will special interest can scroll the data there.
WOCE is major project, investigating the role that the ocean might have on climate, and also how to understand climate variability and climate change, and if possible the human influence.
Therefore during the 1990's the oceans were observed using satellites, floats, data collection through CTD's and XBT's on research ships, also VOS (Voluntary Observing Ships) were used. In addition different numerical models of varying sophistication were employed.
The data so collected can to some extent be compared with the the calcu-

[1] Figures can be found in Chapter 6 of *Ocean Circulation* from *Open University*

lations for volume and heat transports found in this thesis. Although the time interval is around 10 years for WOCE and 150 years for POP, they are still valuable for comparison.
As can be imagined the process that has a major importance for volume and hence heat transports are the ocean circulations from the the equator to the poles. Two major forms of circulation can, as known, be distinguished namely: *Wind-driven* and *Thermohaline*. In this discussion only the former will considered.
As with the circulation in the atmosphere, the wind-driven circulation of the ocean transports heat from lower to higher latitudes. There is though a difference between the two in that the ocean currents have fixed boundaries at the continents. Although it will lead to a tendency of a circular or gyral motion, which is certainly more noticed in the ocean than the atmosphere.
The upper water circulation of the subtropical/mid-latitude Atlantic Ocean consists in its gross features of two great anticyclonic circulations or gyres, *id est* a counterclockwise one in the South Atlantic and a clockwise one in the North Atlantic. Gyres are also present at higher latitudes and will then influence among other things the *Thermohaline Circulation*.
At first sight it might seem appropriate to resemble these two gyres to two gear wheels revolving and meshing near the equator. This, however, gives the impression that one may be driving the other, which is not the case. Rather the two gyres are driven separately, each by the trade winds in its own hemisphere (similar though not identical to those in the Pacific), and they are separated over part of the equatorial zone by the eastward flowing Counter Current.
The Atlantic just north and south of the equator that interests us can be said to extend from 10 °E to 45 °W, a distance of about 6000 km. Concerning ourselves only with the area north of the equator the circulation in the gyre is dominated by the trade winds and of the North Equatoral Current and the part of the South Equatorial Current that flows across the equator. There are also different currents that flow east, that will obviously balance the circulation, like the North Equatorial Counter Current (NECC) and the Equatorial Undercurrent (EUC).
A lot of studies and surveys have been done of the North Atlantic, especially lately and, consequently, different hypothesises about its circulation have developed. What can generally be considered as the classical theory is described in the following.

### 6.12.1 Circulation in the North Atlantic

Svedrup in his book *the Oceans* presented this theory. This has also been done by other authors.
It could be said the anticyclonic circulation (clockwise in the northern hemisphere) is started by the *North Equatorial Current*, which is driven by the north-east trade winds.
It flows west and that part of the South Equatorial current that has crossed the equator joins it. Some of this combined current flow to the the north-west as the *Antilles Current* and the flow is to the east of the West Indies, while some of it flows between the West Indian islands through the Caribbean and the Yucatan Channel into the Gulf of Mexico. From here it slips between Florida and Cuba and then becomes the *Florida Current*. The physical properties of this current seem to indicate that the source is mainly of North and South Equatorial origin, which has been transported across the Caribbean.
Small amounts of the water from the Gulf of Mexico itself appears to be carried out into the Florida Current. Outside the coast of Florida the current is combined with the Antilles Current and from about Cape Hatteras, where the combination breaks away from the North American shore, it is called the *Gulf Stream*. The water of the Florida Current can be distinguished by a salinity minimum due to the Antarctic Intermediate Water transported by the South Equatorial Current. The Antilles Current is composed mostly of the North Atlantic Water and the salinity minimum is much less evident in it. The Gulf Stream flows north-east to the Grand Banks of Newfoundland at about 40 ° N and 50 ° W. From there, the flow which continues east and north is called the *North Atlantic Current*. It then divides and some of it turns north-east between Scotland and Iceland and contributes to the circulation of the Norwegian, Greenland, and Arctic Seas. The remaining part of the North Atlantic Current turns south past Spain and North Africa to complete the North Atlantic Gyre and to feed into the North Equatorial Current. The southward flow covers the greater part of the North Atlantic and is sometimes referred as covering the Sargasso Sea. The flow is so slow and diffuse that it is hard to distinguish specific currents, although the *Canary Current* is recognised flowing to the south off the coast of North Africa.

The boundary currents consists of a western boundary current (known as the *Gulf Stream*) that is swift, deep, and narrow, while the eastern boundary current is slow, diffuse, and broad. The processes involved here are vorticity through wind and friction.
Included in this document is a numerical solution of Stommel's western

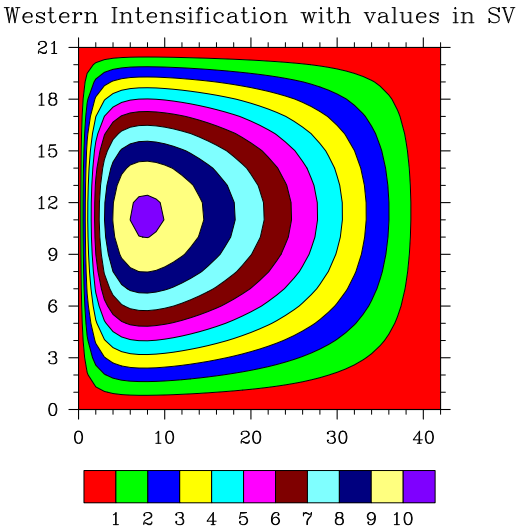


Figure 47: Western Intensification

intensification (Fig 47) performed by the author.
In regards to the Gulf Stream it is known that it attains 150 Sv, as a maximum, as it flows across the Atlantic, most of this is (134 Sv) recirculated and flows south on the the eastern side within the subtropical gyre, which means that a balance of 15 Sv in the upper waters flowing north is quite normal. This is part of what is called MOC (Meridional Overturning Circulation).
The earth is heated by short-wave radiation, that to a great extent falls on tropical regions, and are cooled by outgoing long-wave radiation, which is reasonably uniform over the globe. Measurements from satellites show that the net incoming short-wave radiation at the top the atmosphere exceeds the outgoing long-wave radiation back to space at latitudes equatorialward of about 35 °, so that tropical and subtropical latitudes gain heat from space. At latitudes north of this, heat is lost to space. In order to maintain a heat balance the atmosphere and oceans must transport heat from lower latitudes to higher. The maximum combined atmosphere and ocean heat transport from about 35 ° is about 5.5 PW. Whether the atmosphere or the ocean is the greatest contributor to this transport have been debated by scientists to a great length over the years. So how much the ocean contributes also have great importance how useful the values in this area can be relied upon. Due to this, a recent separation of the total atmosphere plus ocean

energy transport as a function into three different components (ocean heat transport, dry static energy transport, and latent heat transport associated with meridional freshwater transport, which is a combined atmosphere ocean process) indicates that oceans and atmosphere may contribute about equally in maintaining the global heat balance.
In order to access the role that the oceans have in this heat balance equation, three methods have been used lately.

- A *traditional method*, in which bulk formula calculations of atmosphere-ocean heat exchange based on surface observations are integrated over a given surface area to infer the regional ocean heat transport divergence required to balance the atmosphere-ocean heat flux;

- A *residual method*, in which the atmospheric energy transport is subtracted from the incoming short-wave radiation at the top of the atmosphere, in order to arrive at a possible reasonable value for the ocean heat transport;

- A *direct method*, in which the product of ocean velocity and temperature measured over the boundaries of a closed volume are integrated to determine the ocean heat transport divergence for the volume.

Regarding the bulk method the advantage is that it can be applied over arbitrary areas of the ocean, while the disadvantage has been an inability to identify biases in the surface observations or flux parameterisations that make large-area estimates a bit suspicious.
For the residual method its advantage is the availability of satellite radiation measurements of the total ocean plus atmosphere energy transport requirement, while the disadvantage has been that any uncertainty in either the radiation measurements or the atmospheric transport feeds directly into ocean heat transports estimates.
Finally in the case of the direct method the advantage of this method is that it deals with ocean circulation and the mechanisms of ocean heat transport, while the disadvantage has been that direct calculations, could only be made at few locations where high-quality observations were available.
As the model is based on the direct approach for calculating heat transports, which are clearly coupled to volume transports, the understanding of ocean circulation is essential in order to gain knowledge to this connection.
There is a problem to calculate volume, and hence heat transports, for POP within CCSM2. As have been mentioned earlier POP uses a curvilinear grid. The Atlantic Ocean has been assumed to a rectangular grid. This is

probably less of a problem in the South Atlantic, but certainly not in the North Atlantic.
Due to this fact volume and heat transports have to be calculated externally and then used within a Ncl-script, which will be explained a bit later. The external calculation is done by a Fortran program, that has been written in Fortran 90 and it is based on the streamfunction.[2]
Within the project, that led to this master thesis, it had been anticipated that volume and heat transports within and between boxes based on longitude would had been possible to calculate in the North Atlantic.
Due to the above problem this have not been possible, and possible boxes in the North Atlantic can only been based on latitudes. One example of a heat balance based on this has been included in this document.

### 6.12.2 Volume transports from the Equator to 60 °N

At the Equator we will have volume transports between 10.1 to 13.4 Sv (Figures 48 through 51). For this latitude there are no comparable volume transports from WOCE, but there is no reason to assume that the values are not quite reasonable when comparing with higher latitudes.

Moving north to 25 °N latitude the values range from 11 to 15 Sv. WOCE have performed calculations at this latitude and this are in the range 16 $\pm$ 2Sv, which is reasonably close to the range of values calculated from POP. At 45 °N the values lie between 10.5 to 15.5 Sv. Also here WOCE have values that we can use for comparison, this time being in the range 14 $\pm$ 2Sv. This is certainly also within the the range that have been calculated in the POP model.
At the last latitude, which is 60 °N the values range from 7.5 to 9.9 Sv. For this most northern latitude again there are no values to compare with, but as this latitude is outside the subtropical gyral area, it seems to be reasonable that it is a bit lower.

### 6.12.3 Heat transports from the Equator to 60 °N

The Equator have variations between 0.6 and 0.85 PW. Within WOCE there are values just north and south of the Equator, these being between 0.7 PW and 1 PW (Figures 52 through 55). The model also here seem to agree quite well.

Moving to the latitude of 25 °N the values have increased somewhat,

[2] www.ccsm.ucar.edu/models/ccsm3.0/#src

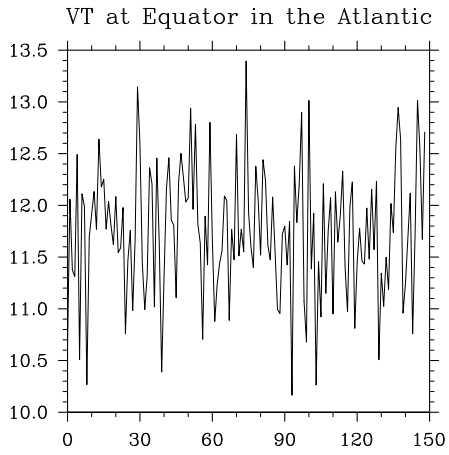


Figure 48: Volume transport at the Equator

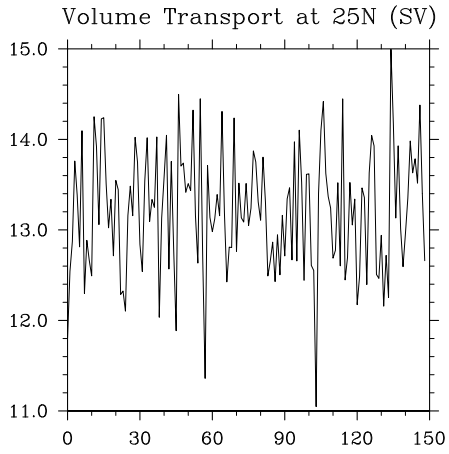


Figure 49: Volume transport at 25N

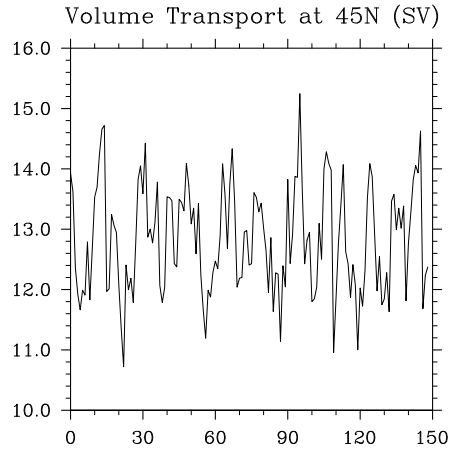


Figure 50: Volume transport at 45N

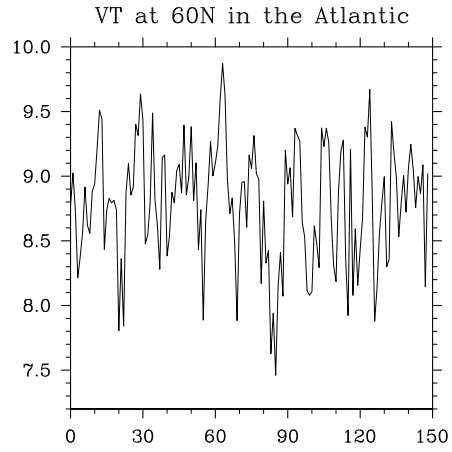


Figure 51: Volume transport at 60N

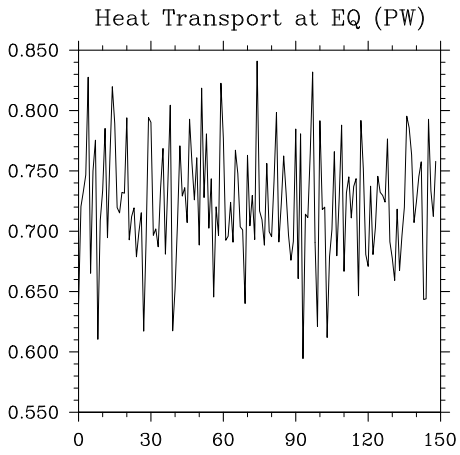


Figure 52: Heat transport at the Equator

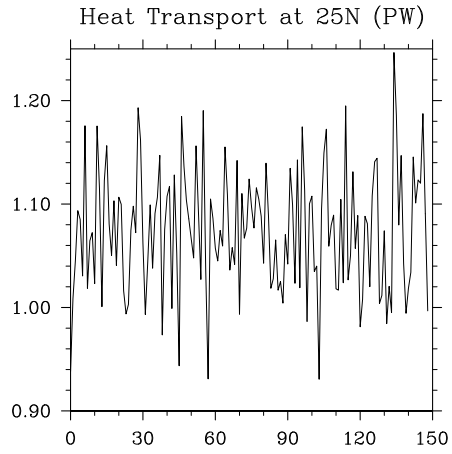


Figure 53: Heat transport at 25N

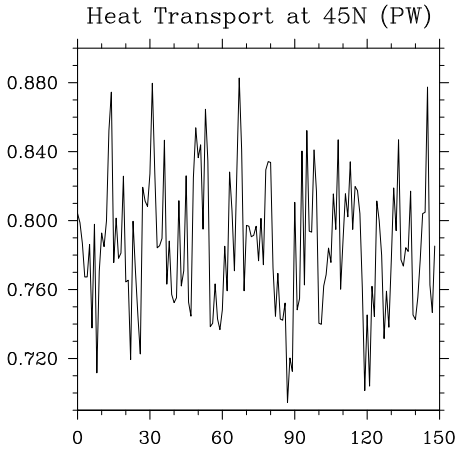


Figure 54: Heat transport at 45N

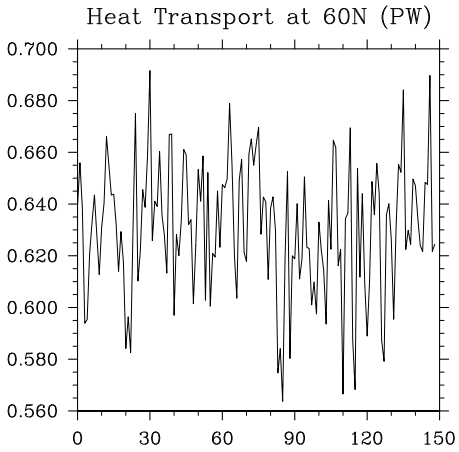


Figure 55: Heat transport at 60N

now ranging from 0.92 to 1.22 PW. The WOCE data here shows about 1.3 PW, while the model data have a maximum value of 1.22 PW and never lower than 0.92 PW. Again it can be said that there is an agreement in value.
In the mid-latitudes the WOCE value is about 0.6 PW, while the POP values are located between 0.71 and 0.88 PW. Even if the values also at this latitude are within a reasonable range, the model displays values up to 0.3 PW higher than WOCE. Although the variations in the model will approach 0.6 PW in those years that the model displays a minimum value, this is no longer the case at the end of the 150 year period.
At this most northern latitude within our calculations, the values display variations between 0.56 and 0.69 PW. These are nearly in the high end 0.4 PW larger than for WOCE. With the knowledge that the model is too warm at this latitude, although it is difficult to know with how much, it would seem that the comparison at this latitude is a bit uncertain.

## 6.13 Heat Balances

One also need to check if the heat transport balances in a box. As an example the box from the Equator to 25N is chosen. Within the the heat-content is calculated (dC/dt). The following figure is then created.

As can be seen there (Fig 56) is a balance here, which seem to show that the calculations of heat transports are fair.

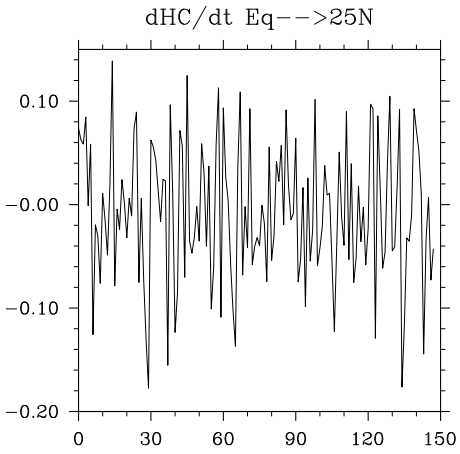


Figure 56: Heat Content Equator to 25N

# 7 Conclusions

This thesis have tried to verify how well the POP model is able to display physical properties and transports in the North Atlantic, especially within the area covered by the western boundary current (the *Gulf Stream*).
As a subtitle reflections have been made to what effect possible changes to the ocean climate, as displayed by the POP model, might have.
As has been described in several topics within this thesis there are primarily two weaknesses that might have important impacts on the results:

- Too warm at 60 °N
- Transports not possible between boxes based on longitude.

The first disadvantage can reasonably well be catered for by making some assumptions, like for instance dividing the changes/anomalies by 2, as they are quite substantial anyway.
With regards to second disadvantage implications are more severe, as it would have been quite useful to get transport values based on longitude as well. As one then can create quite small boxes and investigate how volume and heat moves between boxes.
Sadly enough none of these disadvantages have been changed in CCSM3,

and it could be interesting to follow this up.
Even so, a lot of interesting results have come to light during his study.
The differences in temperature and salinity between Levitus and POP are substantial in several locations.
Temperature anomalies at 25 °N, 45 °N, and 60 °N are very large, and from the model results it must be assumed that the ocean climate might be changing to a large degree. As have been mentioned before an anomaly of at least $\pm 0.1$ is considered to be decisive, and as our values are a lot larger than that, so they should certainly be investigated further.
Volume and heat transports are within the values that one would expect, as volume and heat need to be conserved.
As a final note it could be said the model results show variations that could have a substantial impact on ocean climate and climate in general. This hopefully will lead to further improvements of models and observational methods, in the anticipation that the two worlds of research would cooperate more.

# References


[1] Libes,Susan M: An Introduction to Marine Biogeochemistry, 1992

[2] Millero,Frank J: Chemical Oceanography, 2006

[3] Macdonald, Alison Marguerite: Ocean Fluxes of Mass and Freshwater, PhD dissertation at MIT, 1995

[4] Pond,Stephen and Pickard,George L: Introductory Dynamical Oceanography, ,1983

[5] Knauss,John A: Introduction to Physical Oceanography, 1997

[6] Pedlosky,Joseph: Geophysical Fluid Dynamics, 1979

[7] Gill,Adrian E: Atmosphere-Ocean Dynamics, 1982

[8] Apel,J.R.: Principles of Ocean Physics, 1988

[9] Kundu,Pijush K and Cohen,Ira M: Fluid Mechanics, 2004

[10] Siedler,Gerold etc: Ocean Circulation & Climate, 2001

[11] Fasham, Michael J.R. ed: Ocean Biogeochemistry, 2003